Author(s): Repo, Päivikki & Benick, Jan & Vähänissi, Ville & Schön, Jonas & von Gastrow, Guillaume & Steinhauser, Bernd & Schubert, Martin C. & Hermle, Martin & Savin, Hele

Title: N-type Black Silicon Solar Cells

Year: 2013

Version: Post print

Please cite the original version:

Repo, Päivikki & Benick, Jan & Vähänissi, Ville & Schön, Jonas & von Gastrow, Guillaume & Steinhauser, Bernd & Schubert, Martin C. & Hermle, Martin & Savin, Hele. 2013. N-type Black Silicon Solar Cells. 3rd International Conference on Crystalline Silicon Photovoltaics. Energy Procedia. Volume 38. 866-871. ISSN 1876-6102 (printed). DOI: 10.1016/j.egypro.2013.07.358.

SiliconPV: March 25-27, 2013, Hamelin, Germany

n-type black silicon solar cells

Päivikki Repo[a,]*, Jan Benick[b], Ville Vähänissi[a], Jonas Schön[b], Guillaume von Gastrow[a], Bernd Steinhauser[b], Martin C. Schubert[b], Martin Hermle[b], and Hele Savin[a]

[a]Aalto University, Tietotie 3, 02150 Espoo, Finland
[b]Fraunhofer Institute for Solar Energy Systems, Heidenhofstraße 2, 79110 Freiburg, Germany

---

Abstract

Black silicon is an interesting surface texture for solar cells because of its extremely low reflectance on a wide wavelength range and acceptance angle. In this paper we present how black silicon (b-Si) texturization can be applied on the boron doped front surface of an n-type solar cell resulting in an efficiency of 18.7 %. We show that the highly boron doped emitter can be formed on black silicon without losing its good optical properties and that atomic layer deposited aluminum oxide provides good surface passivation on these boron doped b-Si emitters.

Keywords: black silicon; surface passivation; aluminum oxide; solar cell

---

1. Introduction

Black silicon (b-Si) refers to a nanostructured silicon surface with extremely low surface reflectance. The first application of b-Si was the optimization of etching parameters in a reactive ion etching process (RIE) [1] but later on it became an interesting solar cell surface texture because of its low reflectance on a wide wavelength range and acceptance angle. Besides RIE, other methods for b-Si fabrication, such as laser texturing [2], metal-catalyzed wet chemical etching [3] or plasma immersion ion implantation [4] have been suggested. One issue related to the application of black silicon in an actual solar cell has been the increased surface recombination velocity due to the large surface area of the nanostructure. This causes poor spectral response especially at short-wavelengths [5]. Black silicon has been mostly applied on p-type cells using both thermal oxidation [3] and SiN_x [4, 6] for the front surface passivation. However, the high surface recombination velocity has hindered the gain obtainable from the low reflectance and kept the efficiencies of black silicon cells relatively low, the highest efficiency to date being 18.2 % [7].

In recent years Al_2O_3 has been considered one of the most promising dielectric passivation layers for p- and n-type as well as p^+ surfaces [8]. The passivation ability of Al_2O_3 is related to the combination of low defect density and negative fixed charge at the Si/Al_2O_3 interface. Emergence of ALD into the photovoltaic community has also offered a solution for the surface recombination issue of black silicon

---

* Corresponding author. Tel.: +358504361156
E-mail address: paivikki.repo@aalto.fi

and recent results show that atomic layer deposited aluminum oxide (ALD Al_2O_3) provides good passivation for p-type black silicon surfaces [9-10].

2. Experimental details

2.1. Solar cell process

PERL (passivated emitter with rear locally diffused) solar cells with black silicon on the front surface were fabricated on n-type 5 Ωcm FZ (400 µm) silicon wafers. The solar cell structure and the main process steps are shown in Figure 1. Reference cells with inverted pyramids and an Al_2O_3/SiN_x stack on the front surface were processed alongside with the black silicon cells featuring only Al_2O_3 at the front. The only difference in the reference cell process was the front surface texturization and the deposition of 65 nm of SiN_x with plasma enhanced chemical vapor deposition (PECVD). The process was started with a masking oxidation to define the cell areas of 2×2 cm^2. Black silicon was etched on the window areas with a cryogenic deep reactive ion etching process at -120 °C using SF_6/O_2 plasma. Etching of 7 minutes leads to a random nanostructure shown in Figure 2a with an average pillar height of 1 µm and width of 200 nm.

Boron emitters were formed in a BBr_3 tube furnace diffusion at three different temperatures: 890 °C, 910 °C and 930 °C. For the front surface passivation 10 nm of Al_2O_3 was deposited with plasma assisted atomic layer deposition (PA-ALD) whereas for the rear surface passivation the *PassDop* [11] process was applied. This includes the deposition of phosphorus doped amorphous SiC_x:H with PECVD and the opening of point contacts through the passivation layer with a laser. During the laser process the phosphorus creates a local back surface field under the contact points. The rear surface metallization was done with evaporated aluminum followed by an anneal at 425 °C for 15 minutes to activate the Al_2O_3 passivation. The front surface contact grid was defined by photolithography and the contacts were formed by evaporated Ti/Pd/Ag thickened with electroplated Ag.

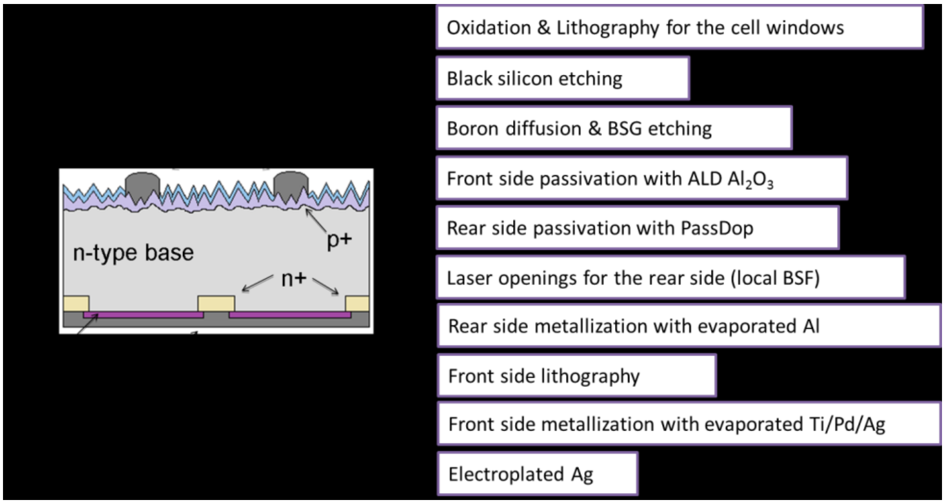

Fig. 1. Schematic of the applied solar cell structure and the main steps of the cell process.

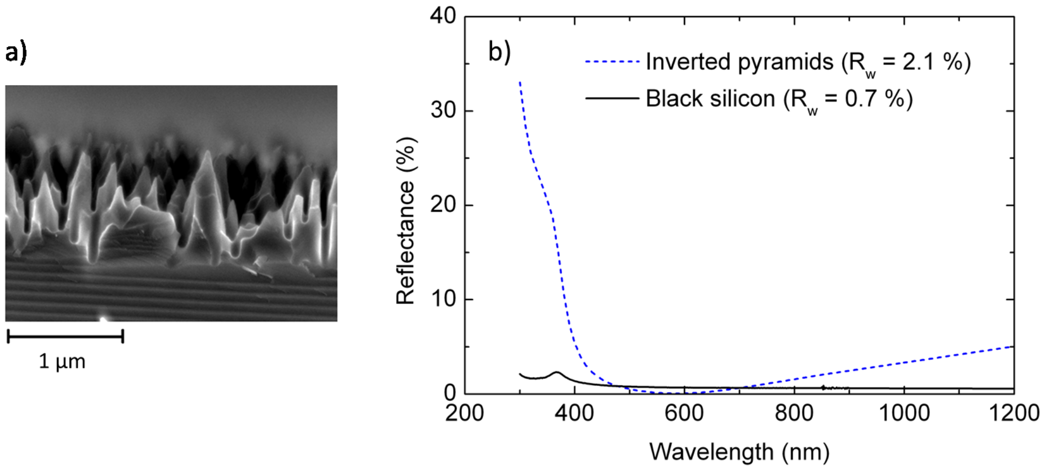

Fig. 2. (a) Scanning electron microscope (SEM) image of a black silicon surface directly after etching. (b) The reflectance of black silicon after emitter formation at 910 °C, boron glass etching and Al_2O_3 deposition. As a comparison the reflectance from a cell with inverted pyramids and Al_2O_3/SiN_x stack on the front surface (the reflectance of the contacts is omitted). The escape reflection is removed from the curves by assuming the front surface reflectance to be linear for $\lambda > 900$ nm and by extrapolating the measured reflectance. The AM1.5G spectrum weighted average reflectances are calculated by taking into account only the surface reflectance.

3. Results and discussion

Figure 2b presents an example of b-Si reflectance after emitter diffusion at 910 °C and the following Al_2O_3 deposition. As a comparison the reflectance from inverted pyramids with an Al_2O_3/SiN_x stack is shown. In the short wavelength range the b-Si reflectance is much lower than in the reference samples whereas in the mid-wavelength range the reference sample exhibits slightly smaller reflectance values. The AM1.5G spectrum weighted average reflectance calculated from the front surface reflectance is however smaller in the black silicon sample even after processing and only with Al_2O_3 on the front surface.

The solar cell parameters measured at one-sun with an aperture area of 4 cm^2 as well as the pseudo fill factors are shown in Table 1. All cells, including the reference cell, exhibit a relatively low open-circuit voltage of ~630 mV. The comparison with the IQE reveals that all cells suffer from an insufficient rear side passivation. This is mainly due to the fact that the processing sequence was not adopted to meet the temperature requirements of both, the front side Al_2O_3 as well as the rear side *PassDop* layer, i.e. the high temperature applied for the annealing of the Al_2O_3 degraded the rear side passivation. The front side passivation, nevertheless is quite effective for all cells, as can be seen by the high IQE in the short wavelength range. This is coherent with our previous study on the surface passivation of boron doped b-Si emitters where a J_{0e} value of 51 fA/cm^2 was reached indicating an efficient surface passivation also on p^+ surfaces on an n-type substrate [12]. The J_{0e} values were extracted from the quasi-steady-state photoconductance measurements (QSSPC, Sinton WCT-120) from symmetrical emitter samples by using the high injection method [13]. Nevertheless, the highest IQE is reached with the reference cells. For the b-Si cells the IQE reduces with increasing diffusion temperature. An adoption of the diffusion process might increase the IQE to the same level as the reference cells.

The reference cell with the inverted pyramids shows the highest short-circuit current of 39.9 mA/cm^2. The short-circuit current of the black silicon cells is slightly lower and shows a small dependence of the diffusion temperature: the higher the diffusion temperature i.e. the deeper and more highly doped the emitter, the smaller the short-circuit current density, as also can be seen in the IQE. Omitting the effect of the reflectance from the contacts the black silicon cells exhibit an average reflectance (R_w) of ~2-3 % which is higher than could be expected although still comparable to the average reflectance of the reference cells (see Figure 3). This naturally plays a role in the relatively low J_{sc} values. However, the problem causing the higher reflectance values has been identified and is easily avoided in future processing.

The fill factor of all cells is relatively low. The root cause of this needs to be further investigated. As can be seen in the SEM image in Figure 4 showing a cross section of the b-Si surface under the evaporated metal contact the metal does not reach the extremely small gaps on the b-Si surface which might lead to an increased series resistance. However, also the reference cells suffer from a low FF. This can be related to the used base material with relatively high resistivity but more experiments are needed to have a more thorough analysis. The pseudo fill factor values are also lower than expected indicating that the low FF values cannot be completely explained by a high series resistance. No shunting could be observed based on the IV characteristics. Adoption of the cell processing to the b-Si process will allow much higher efficiencies in the future.

In total a cell efficiency of 18.7% could be reached for these very first n-type b-Si cells. This proves that b-Si is a promising approach for the front side texturing. Most importantly we have been able to show that the nanostructured front surface is not destroyed during the multiple processing steps including diffusion, boron glass etching as well as resist application and stripping needed in lithography.

Table 1. The solar cell parameters from the three different black silicon cells and the reference cell with inverted pyramids measured at one sun. The pseudo fill factors (PFF) were measured with Suns-V_{oc}. Cell area is 4 cm^2.

Surface structure	Diffusion T (°C)	J_{sc} (mA/cm^2)	V_{oc} (mV)	PFF (%)	FF (%)	η (%)
Black silicon	890	39.3	628	80.1	75.8	18.7
Black silicon	910	39.2	632	79.8	75.8	18.7
Black silicon	930	38.4	630	80.3	76.1	18.4
Inverted pyramids	910	39.9	631	77.2	75.3	18.9

In order to optimize the emitter diffusion process for a black silicon surface it is important to gain more information about the emitter profile. This has already been and will further be addressed with process simulations whereas measuring the profile might prove to be unfeasible. Optimizing the emitter profile relates to the optimization of the surface passivation and the metallization and especially the metallization should be further addressed. The annealing treatments required by the Al_2O_3 and the *PassDop* passivation should also be fitted to the process accordingly.

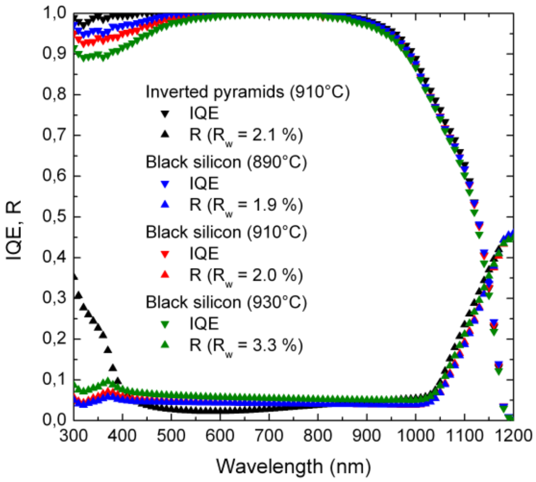

Fig. 3. The internal quantum efficiencies (IQE) and reflectances (R) of the different black silicon cells and the reference cell with inverted pyramids and an Al_2O_3/SiN_x stack. Spectrum weighted average reflectances (R_w) were calculated by taking into account only the front surface reflection although the escape is still shown in the figure. The reflection from the contacts was also omitted in the R_w calculation.

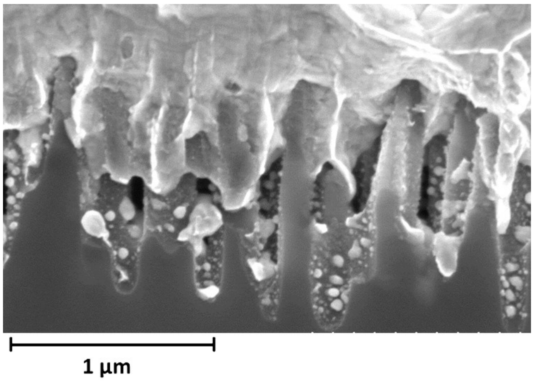

Fig. 4. A SEM image of the black silicon and front metal contact interface showing how the metal is mostly deposited on the nanostructure and does not reach the valleys of the structure.

4. Conclusions

We have shown that black silicon passivated with ALD Al_2O_3 can be applied on the highly boron doped front surface of an n-type PERL solar cell. The best black silicon cells show an efficiency of 18.7 %. The high IQE in the short wavelength region proves the effective passivation of the boron doped black silicon surfaces with the PA-ALD Al_2O_3. We were able to show that the nanostructured front surface is not destroyed during the multiple processing steps including diffusion, boron glass etching as well as resist application and stripping needed in lithography. With more process optimization considerably higher efficiencies can be expected. These optimization steps include the careful consideration of the diffusion process as well as the front surface passivation and contact formation. However, as the first trial in introducing Al_2O_3 passivated black silicon to an n-type solar cell the results are promising.

Acknowledgements

The authors thank Sonja Seitz, Felix Schätzle, Karin Zimmermann, Jutta Zielonka, Ulrich Jäger, Nicolas König, Nicole Hennig and Elisabeth Schäffer from Fraunhofer ISE for the support with processing and characterization and acknowledge the provision of facilities and technical support by Aalto University at Micronova Nanofabrication Centre. P. Repo acknowledges the Graduate School of the Faculty of Electronics, Communications and Automation for the financial support.

References

[1] Jansen H, de Boer M, Legtenberg R, Elwenspoek M. *J. Micromech. Microeng* 1995; **5**: 115-120.

[2] Halbwax M, Sarnet T, Delaporte PH, Sentis M, Etienne H, Torregrosa F, Vervisch V, Perichaud I, Martinuzzi S. *Thin Solid Films* 2008; **516**: 6791-6795.

[3] Koynov S, Brandt MS, Stutzmann M. *Phys. Stat. Solidi RRL.* 2007; **1**: R53-R55.

[4] Xia Y, Liu B, Liu J, Shen Z, Li C. *Sol. Energy* 2011; **85**: 1574-1578.

[5] Yuan HC, Yost VE, Page MR, Stradins P, Meier DL, Branz HM. *Appl. Phys. Lett.* 2009; **95**: 123501.

[6] Dimitrov DZ, Du C-H. *Surf. Sci.* 2012 ; Accepted for publication.

[7] Oh J, Yuan H-C, Branz HM. *Nature Nanotechnology* 2012; **7**: 743-748.

[8] Dingemans G, Kessels WMM. *Journal of Vacuum Science and Technolog y A* 2012; **30**: 040802.

[9] Repo P, Haarahiltunen A, Sainiemi L, Yli-Koski M, Talvitie H, Schubert MC, Savin H. *Journal of Photovoltaics* 2012; **3**: 90-94.

[10] Otto M, Kroll M, Käsebier T, Salzer R, Tünnermann A, Wehrspohn RB. *Appl. Phys. Lett.* 2012; **100**: 191603.

[11] Suwito D, Jäger U, Benick J, Janz S, Hermle M, Glunz SW. *IEEE Transactions on Electron Devices* 2010; **57**: 2032-2036.

[12] Repo P, Benick J, Vähänissi V, Schön J, Schubert MC, Hermle M, Savin H. To be submitted to Appl. Phys. Lett.

[13] Kane DE, Swanson RM. *Proceedings of the 18th IEEE Photovoltaic Specialists Conference* 1985, Las Vegas, (IEEE, New York, 1985): 578-583.